AD-A069 176 DELAWARE UNIV NEWARK F/G 7/2
THE EFFECT OF HEAT TREATMENT ON THE NEAR BAND EDGE PHOTOCONDUCT--ETC(U)
JUL 74 G M STORTI, K W BOEER N00014-71-C-0169
UNCLASSIFIED NL

| OF |
AD
A069176

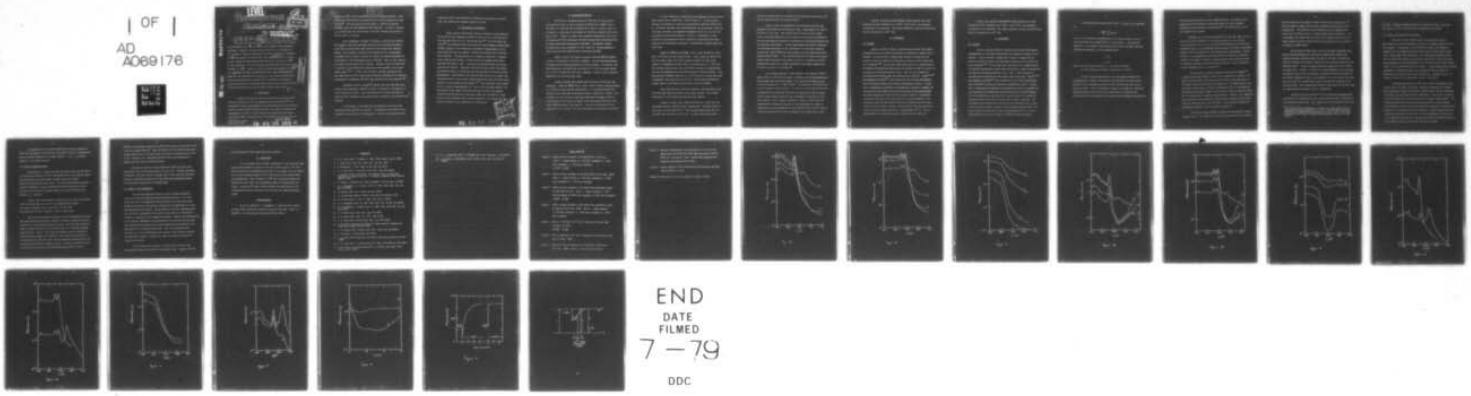

END
DATE
FILMED
7-79
DDC

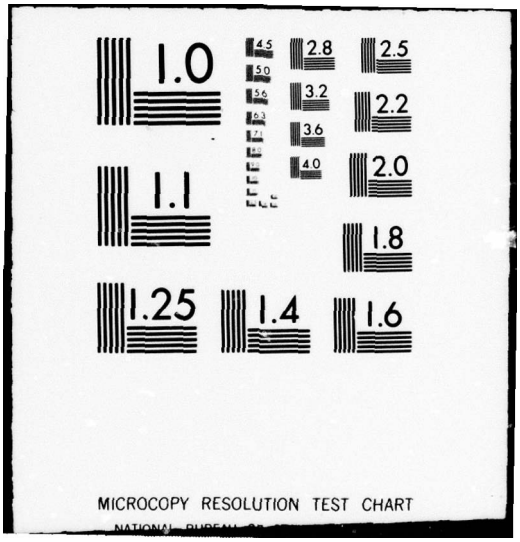
1.0
1.1
1.25
1.4
1.6
1.8
2.0
2.2
2.5
2.8
3.2
3.6
4.0
4.5
5.0
5.6
6.3
7.1
8.0
MICROCOPY RESOLUTION TEST CHART

LEVEL II

The Effect of Heat Treatment on the Near Band Edge Photoconductivity of Class I CdS Crystals+

by

G. M. Storti and K. W. Böer
University of Delaware, Newark, DE 19711

Contract N00014-71-C-0169
Status Rept. No. 15,
1 May - 31 Jul 74,
31 Jul 74
31 p.

Abstract

The near band edge photocurrent structure of Class I CdS crystals was investigated near 77°K and 295°K by use of double beam illumination techniques. Changes in the photocurrent structure as a consequence of heat treatment, infra-red illumination and oxygen backfill were measured. At 98°K, quenching of the photocurrent near 5000 Å observed in a virgin crystal changed into photocurrent maxima after heat treatment to 175°C. At room temperature, the near band edge quenching remained even after heat treatment to 175°C. Visible and infra-red excitation ranging from 0.6 μm to 1.5 μm always strongly quenched the near band edge photoconductivity maxima but had considerably less influence on the intrinsic photocurrent. The currently-used model to explain Class I properties is expanded to include the influence of the space-charge region in which the photocurrent flows and an acceptor-level with multiply charged energy states.

1. Introduction

A useful classification scheme for characterizing certain photoelectronic properties of CdS was suggested by Gross and Novikov[1] as a consequence of their investigations of the photoconductivity and absorption spectra at liquid nitrogen temperature (LNT). Two types of crystals were distinguished - Class I, in which the spectral dependence of the photoconductivity (SDP) is coincident with the absorption spectrum and Class II

+Part of Ph.D. Thesis
*Supported by ONR

in which the SDP is anti-coincident with the absorption spectrum. These results have been explained satisfactorily in a model presented by Voigt and Ost.[2] The main feature of this model is a position dependent lifetime, $\tau_n(x)$, for the conduction band electrons. In Class I crystals, τ_n is greater near the surface than in the bulk, whereas the reverse is true for Class II crystals.

As a consequence, in Class II crystals, a photocurrent maximum will appear to the long wavelength side of the free exciton absorption lines (the so-called false peak) because of the greater bulk lifetime. However, there should be no photocurrent maximum in the corresponding wavelength range in Class I crystals as long as the spatial dependence of the lifetime is the determining factor in the SDP. This, in fact, appears to be the case with many Class I crystals. However, there are other Class I crystals in which photocurrent maxima have been observed in this wavelength range.[2-7]. In fact, even in Class I crystals showing no near band edge structure under single beam excitation, quenching of an intrinsic photocurrent by additional near band edge excitation has been reported.[8]

Bragagnolo, Storti, and Böer[7] showed that near band edge photocurrent maxima appeared in the SDP of Class I crystals as a consequence of a heat treatment at 180°C. Also, they observed the strong influence of infra-red (IR) illumination and oxygen surface coverage on this photocurrent spectrum.

In this paper, a more detailed investigation of the near band edge photocurrent spectrum is reported. In particular, the effect of heat treatment on the spectrum is investigated. Crystals are probed with both

single and double beam excitation to bring out characteristic features. Also, the influence of adsorbed oxygen is studied.

2. Experimental Arrangement

Single crystal CdS platelets having a thickness of approximately 100 μm and an areal dimension of about 0.5 cm^2 (.5 cm x 1 cm) were grown from the vapor phase in a N_2 - H_2S carrier gas.[9] Two Ti-Al ohmic contacts[10] were evaporated onto one of the two major surfaces [$(11\bar{2}0)$ plane] thereby creating a slit between the electrodes of approximately 0.5 cm across which 20 volts was applied. Current was measured with a Keithley 409 Picoammeter. The photocurrent was excited by light from a tungsten source which passed through a 1-meter Jarrel-Ash scanning spectrometer (spectral band width ≤ 4 Å). A polarizer was placed between the spectrometer and the crystal. Additional excitation of the crystal with either un-polarized visible or infra-red light was provided by a Bausch and Lomb monochromator. Measurements of the photocurrent were made at either room temperature (RT) or near liquid nitrogen temperature (LNT) with the crystal mounted in an ultra-high vacuum chamber.[11] Heat treatments were carried out in a vacuum of approximately 10^{-7} torr in the following fashion: The temperature of the copper block onto which the crystals were pressed (insulated from the block by a thin mica sheet) was increased at a rate between 5 and 10°C/minute until a given temperature was reached and then rapidly quenched to room temperature (~ 30°C/minute).

3. Experimental Results

The SDP of an untreated crystal at 98°K and 10^{-8} torr excited with polarized light is seen in Figures 1a ($\vec{E}\|\vec{C}$) and 1b ($\vec{E}\perp\vec{C}$), curve 1. The effect of step-wise heat treatments up to 175°C is seen in curves 2-4 of Figure 1. Relatively little change in the SDP was observed after treatment at 75°C. However, at higher heat treatment temperatures, the intrinsic photocurrent first decreased and then increased while the photocurrent at longer wavelengths monotonically increased. Considerable changes occurred after a heat treatment at 175°C (curve 4). Maxima appeared at 4900 Å and 4940 Å for $\vec{E}\|\vec{C}$ and 4935 Å and 4965 Å for $\vec{E}\perp\vec{C}$.

Figure 2 shows the changes occurring in the SDP ($\vec{E}\|\vec{C}$) measured at RT as a consequence of the heat treatments. The intrinsic photocurrent increased with increasing temperature of heat treatment. In addition, the dark photocurrent increased from less than 10^{-12} A for the virgin crystal to $\approx 4 \times 10^{-9}$ A after the 175°C heat treatment. Little, if any, structure appeared in the near band edge range.

Changes observed under double beam excitation at 98°K were very pronounced. Figure 3a ($\vec{E}\|\vec{C}$) and 3b ($E\perp C$), curves 1-3 show strong quenching of a 4500 Å bias photocurrent (indicated by -- at the right edge of the figure) by near band edge illumination between $\sim$ 4900 Å and $\sim$ 5100 Å. Heat treatment at 175°C (curve 4) caused the quenching to disappear and two distinct photocurrent maxima to appear at the wavelengths observed in the single beam experiments (see Figure 1). The near band edge photocurrent maxima in curve 4 occurred at the same wavelengths as the strongest quenching.

At room temperature, quenching was also apparent in the near band edge range between ~ 5000 Å and ~ 5400 Å (Figure 4). In the untreated crystal, the maximum was centered at approximately 5200 Å for $\vec{E} \| \vec{C}$ (curve 1). With heat treatment, the quenching became less pronounced. After the 175°C heat treatment, the quenching disappeared (curve 4), but was still noticeable in the kinetic behavior - that is, a substantial initial decrease in the photocurrent level occurred on illumination with 5200 A light but was followed by a recovery to a photocurrent slightly above the bias level.

Figure 5a ($\vec{E} \| \vec{C}$) and 5b ($\vec{E} \perp \vec{C}$), curve 1 shows the SDP at ~ 87°K and 2×10^{-3} torr for the virgin crystal. Curve 2 shows the SDP at 87°K for the crystal after 175°C heat treatment, backfill of the vacuum chamber to atmospheric pressure with O_2, and pump down to 2×10^{-3} torr. The intrinsic photocurrent levels after heat treatment are approximately one order of magnitude less than they were prior to heat treatment. Also, the post heat treatment levels at ~ 2×10^{-3} torr are an order and a half in magnitude lower than that at 10^{-8} torr. The extrinsic photocurrent maxima remain at the higher pressure after the heat treatment.

With additional bias excitation (4500 Å), some quenching in the near band edge range was present in the virgin crystal. For the heat treated case, the extrinsic photocurrents were additive.

Figure 6, curves 1 and 2 show the RT SDP at 2×10^{-3} torr for the virgin and heat treated crystal, respectively. The dark current in both cases was less than 10^{-12} A. The intrinsic photocurrent was considerably less than that at 10^{-8} torr. In double beam measurements, a

4500 Å bias photocurrent was quenched by near band edge illumination both for the virgin and the heat treated crystal.

Figure 7 shows the quenching of the principal near band edge maximum by broad band red and infra-red light. Measurements were made at 87°K and 2×10^{-3} torr. SDP at 87°K and 10^{-3} torr by 0.85 μm light. Curve 1 is without additional IR and curve 2 is with the IR illumination. The near band edge photocurrent was quenched to a much greater degree than the intrinsic photocurrent. Further measurements were made to determine the wavelength dependence of the quenching of the B_1 exciton intrinsic photocurrent (4850 Å $\vec{E}11\vec{C}$) and the principal near band edge photocurrent maximum (4933 Å, $\vec{E}11\vec{C}$). It was observed that the B_1 exciton photocurrent showed slight quenching in the range 0.6 μm to 1.1 μm while the 4933 Å photocurrent maximum was strongly quenched by wavelengths ranging from 0.6 μm to at least 1.5 μm (Figure 8).

It was found necessary to pre-illuminate the crystal at 4933 Å (E11C, 87°K, 2×10^{-3} torr) in order to develop fully the photocurrent of the principal near band edge maximum. This could not be done by prior intrinsic illumination ($\lambda < 4860$ Å, $\vec{E}11\vec{C}$). The build-up of the photocurrent at 4933 Å required several minutes. If, then, the crystal was intrinsically illuminated for one-half-hour and then re-illuminated at 4933 Å, photocurrent steady state occurred at this wavelength of excitation in less than a minute. This is shown in Figure 9. However, either infra-red illumination or warming the crystal to room temperature was found to necessitate the pre-illumination at 4933 Å ($\vec{E}11\vec{C}$, 87°K, 2×10^{-3} torr) to restore the photocurrent at this wavelength to its steady state value.

Finally, the intrinsic photocurrent varied linearly with light intensity for heat treatments up to 125°C. Above 125°C, the dependence was observed to be sublinear. The linear dependence returned on backfilling with O_2 and pump-down to 10^{-3} torr.

4. Discussion

4.1 General

Previous studies on Class I crystals have indicated that spatial inhomogeneities in the defect distribution are required to explain Class I behavior. On the one hand, a higher donor density is needed near the surface in order to explain the substantial increase in dark current with heat treatments.[12] On the other hand, there has to be a higher density of effective recombination centers near the surface in order to explain the the shape of the photoconductivity curve - that is, the lifetime for electrons must be greater near the surface than in the bulk. Weber[13,14] and Bragagnolo and Böer[11] have treated the case in which band bending near the surface provides the necessary recombination centers. In this case, a homogeneous distribution of recombination centers is assumed, but only those near the surface are sensitized because of the band bending. The other possibility is that there are a greater number of recombination centers near the surface than in the bulk due to growth conditions. The experiments that have been reported above do not differentiate as to which of the two is most likely. However, they do indicate that the width of the layer in which the photocurrent flows is approximately 10^{-5} cm - that is, approximately the extinction length for maximum intrinsic absorption.

Finally, the intrinsic photocurrent varied linearly with light intensity for heat treatments up to 125°C. Above 125°C, the dependence was observed to be sublinear. The linear dependence returned on backfilling with O_2 and pump-down to 10^{-3} torr.

4. Discussion

4.1 General

Previous studies on Class I crystals have indicated that spatial inhomogeneities in the defect distribution are required to explain Class I behavior. On the one hand, a higher donor density is needed near the surface in order to explain the substantial increase in dark current with heat treatments.[12] On the other hand, there has to be a higher density of effective recombination centers near the surface in order to explain the the shape of the photoconductivity curve - that is, the lifetime for electrons must be greater near the surface than in the bulk. Weber[13,14] and Bragagnolo and Böer[11] have treated the case in which band bending near the surface provides the necessary recombination centers. In this case, a homogeneous distribution of recombination centers is assumed, but only those near the surface are sensitized because of the band bending. The other possibility is that there are a greater number of recombination centers near the surface than in the bulk due to growth conditions. The experiments that have been reported above do not differentiate as to which of the two is most likely. However, they do indicate that the width of the layer in which the photocurrent flows is approximately 10^{-5} cm - that is, approximately the extinction length for maximum intrinsic absorption.

The photocurrent obtained from a Class I crystal can be expressed as

$$I = \frac{e\mu FA}{L} \int_0^L n(x)\, dx$$

where x is the dimension perpendicular to the crystal surface, A is the cross-sectional area through which the current flows, μ, the electron mobility, F, the electric field between the contacts, and n(x), the free electron concentration, can be determined from

$$n = a\tau_n$$

$$\partial = \beta k I$$

where a is the excitation density, τ_n, the electron lifetime.

For the subsequent discussion, steady state is assumed.

For the intrinsic photocurrent, the excitation mechanisms are straightforward - namely, either band to band excitation or free exciton absorption with subsequent ionization of the electrons and holes to the respective bands. This is indicated as process 1 in Figure 10. Near band edge photocurrents (other than those seen in Class II crystals) are usually associated with bound exciton formation with subsequent dissociation

of the electrons and holes into the respective bands. The bound exciton mechanism has the advantage of potentially high oscillator strengths (reflected in high absorption coefficients)[15] and deep levels at which the excitons can be formed.

Quenching of an intrinsic photocurrent by near band edge excitation and the subsequent appearance of photocurrent maxima on heat treatment having magnitudes close to that of intrinsic photocurrents (for absorption constants likely to be considerably less than that for intrinsic absorption) indicate that the excitation is also affecting the recombination. Because of this, it is suggested that the bound exciton is formed at an acceptor. Further, the acceptor can exist in various charge states that are located at different energetic positions within the band gap. (For a discussion of multi-charged centers, see Ryvkin.[16])

Following ideas initially formulated by Halsted and Segall[17] to explain green edge emission in CdS, the bound exciton is formed at the singly ionized acceptor levels and then dissociates, releasing a hole to the valence band and converting the acceptor into the doubly-ionized state. The doubly ionized state is located energetically close to the conduction band (Halsted and Segall suggest a level 0.09 eV from the conduction band), but is surrounded by a repulsive coulomb barrier. However, it is suggested that an electron can be thermally released from the doubly ionized center into the conduction band at LNT and above. This excitation mechanism is indicated by processes 2 and 3 as shown in Figure 10.

Electrons and holes normally recombine through the multi-charged acceptor levels. For example, a hole from the valence band can recombine

with an electron in the singly or doubly ionized state converting it to the un-ionized or singly ionized state, respectively (processes 4 and 5, respectively). The electron in the conduction band can recombine and convert the un-ionized state to a singly-ionized state (process 6). It is considerably less likely that an electron will recombine and convert the singly-ionized state to a doubly-ionized state because of the presence of a repulsive coulomb barrier.

On the basis of these ideas, the near band edge quenching occurs because holes produced by the excitation recombine more rapidly with electrons from the conduction band (provided by intrinsic illumination) than the electrons in the doubly ionized state are thermally excited to the conduction band.* A near band edge maxima will appear when this criteria no longer holds. However, it can be of the same magnitude as the intrinsic photocurrent only if the recombination is modified by the deactivation of the normal recombination path. The appearance of a hole trap on heat treatment can result in a significantly greater lifetime for electrons in the conduction band. Hole trapping and electron recombination at the hole trap are represented by processes 7 and 8, respectively.

Chemeresyuk and co-workers[20-22] have noted both negative photoconductivity and quenching of a bias intrinsic photocurrent in CdSe due to near band edge illumination. This suggests that the phenomena involved are

*This criteria must be fulfilled if quenching of a bias photocurrent in negative photoconductivity[18] is to occur. Bube[19] points out that conditions for negative photoconductivity are most easily fulfilled by centers that have singly or doubly charged negative states for n-type material.

the same. Transient quenching behavior as observed by them in CdSe and Gutsche et. al.[22] in CdS can also be explained by this model.

4.2 Effect of Vacuum and Heat Treatment

Initially, for the virgin crystal, the dark Fermi level is positioned very near the energetic position of the singly charged state of the acceptor. Consequently, in the unexcited crystal, the acceptor is primarily in the un-ionized state with some centers in the singly-ionized state. With single beam illumination, the intrinsic photocurrent levels are low because the crystal is relatively unsensitized. Little near band edge quenching is observable because of the relative lack of singly ionized states at which bound excitons can be formed. A linear photocurrent-intensity dependence is observable because the illumination does not affect the population of centers in the un-ionized state (τ_n = constant since p_r, the density of holes in the recombination centers, is constant).

Decreasing the pressure to 10^{-8} torr and heat treatments at this pressure have the effect of driving electrons associated with adsorbed gases (primarily oxygen) into the near surface region, thereby sensitizing this region and increasing the dark conductivity. This causes a decrease in the un-ionized states and an increase in the singly ionized states. The intrinsic photocurrent increases and quenching effects become greater. The subsequent decrease of the quenching and the appearance of photocurrent maxima at $\sim$ LNT indicate that heat treatments at higher temperatures have caused the formation of a hole trap. At room temperature, the hole trap is not effective (the trap is in thermal contact with the valence band), so that quenching remains even for the 175°C heat treatment.

The appearance of a non-linear photocurrent-intensity dependence after heat treatment at 175°C is due to the number of holes in recombination centers becoming dependent on the light intensity - that is, τ_n becomes dependent on the light intensity.

4.3 Effect of Oxygen Backfill

Reintroduction of oxygen decreases the dark current and the intrinsic photocurrent because of the de-sensitization of the near surface region. The chemisorption of oxygen removes electrons from this region, thereby lowering the dark Fermi level. The linear photocurrent-excitation intensity dependence is again observable because the density of the un-ionized state of the multi-charged acceptor is little affected by illumination (τ_n = constant).

However, the reintroduction of oxygen does not affect the presence of the near-band edge maxima at LNT in the photocurrent spectra. This further indicates that a new center, the hole trap, was produced by the heat treatment at 175°C in high vacuum.

The fact that prolonged illumination at the wavelength of the near band edge photocurrent maxima is required to obtain a steady-state value is indicative of the competing processes involved. Near band edge excitation tends to reduce the density of un-ionized states of the multiply charged acceptor levels - that is, the normal recombination path for conduction band electrons no longer is as effective. The excitation also tends to re-route holes into the hole traps, thereby enhancing recombination of the conduction band electrons through this path. Intrinsic illumination prior to the build-up of the near-band edge photocurrent maxima is not as

effective in producing trapped holes because the density of un-ionized states is not as strongly affected. After the build-up of the near-band edge photocurrent maxima, holes in the hole traps can remain for long periods of time at LNT. Therefore, the subsequent build-up time of the photocurrent is shorter than that for the initial build-up.

Heating the crystal to room temperature ionizes the hole traps. Consequently, no near-band edge maxima are seen at RT. Instead, quenching is observed. When the crystal is brought back to LNT, the same excitation process is necessary to build-up the near band edge photocurrent maxima; in other words, holes have to be trapped again.

4.4 Effect of IR Illumination

The near-band edge photocurrent was more strongly quenched by infra-red illumination than the intrinsic photocurrent was. It is most likely that the IR illumination excites the holes out of the hole traps, thereby de-activating a key process necessary for the appearance of a near-band edge photocurrent maxima. The prevention of the hole trapping process can also cause a quenching of the intrinsic photocurrent if the electron lifetime is dependent on the trapped hole density. However, the dissimilarity of the spectral dependence of the quenching of the intrinsic and near-band edge photocurrents indicates that another mechanism may be dominant in the quenching of the intrinsic photocurrent. This could possibly be the activation of a fast recombination path similar to that commonly reported for CdS single crystals. Further work needs to be done to clarify the transitions involved.

The fact that it is necessary to build-up the near band edge photocurrent maxima at LNT after IR illumination also supports the idea

of the existence of hole traps after heat treatment.

5. Conclusions

It is concluded that the defect responsible for the near band edge photocurrent behavior is located in the near surface region ($\approx 10^{-5}$ cm). Both excitation and recombination processes are associated with this defect. It is a multi-charged acceptor with at least three states located within the forbidden gap. Heat treatment at 175°C and low pressure causes the formation of hole traps that considerably modify the recombination processes. Adsorption of oxygen further enhances the modification of the recombination processes associated with the near band edge photocurrent maxima.

Acknowledgments

We wish to thank Drs. J. Bragagnolo, J. Phillips and H. Hadley for many useful discussions during the course of this work. Also, we thank Dr. L. van den Berg for growing the CdS platelets.

References

1. E. F. Gross and B. V. Novikov, J. Phys. Chem. Solids, 22, 87 (1961)
2. J. Voigt and E. Ost, Phys. Stat. Sol., 33, 381 (1969).
3. H. Mitsuhaski, J. Phys. Chem. Solids, 22, 223 (1961).
4. Y. S. Park and D. C. Reynolds, Phys. Rev., 132, 2450 (1963).
5. Y. Fujishvio and H. Mitsuhashi, Proceedings of the International Conference on Luminescence, Ed., G. Szigeti, Akadémiai Kiadó, Budapest 1968 (p. 1056).
6. K. Colbow, A. Jmaeff and K. Yuen, Canadian J. of Phys. 48, 57 (1970).
7. J. A. Bragagnolo, J. M. Storti, and K. W. Böer, Phys. Stat. Sol. (a) 22, 639 (1974).
8. L. Grabner, Phys. Rev. Letters 14, 551 (1965).
9. L. van den Berg, Master's Thesis, University of Delaware, 1972.
10. K. W. Böer and R. B. Hall, J. Appl. Phys. 22, 75 (1966).
11. J. A. Bragagnolo and K. W. Böer, Phys. Stat. Sol. (a) 21, 291 (1974).
12. J. A. Bragagnolo, C. Wright, and K. W. Böer, Phys. Stat. Sol. (a), 24, 147 (1974).
13. E. H. Weber, Phys. Stat. Sol., 28, 649 (1968).
14. E. H. Weber, Phys. Stat. Sol. (a) 1, 665 (1970).
15. C. H. Henry and K. Nassau, Phys. Rev. B 1, 1628 (1970).
16. S. M. Ryvkin, Photoelectric Effects in Semiconductors, Chapter VII, Consultants Bureau, New York 1964.
17. R. E. Halsted and B. Segall, Phys. Rev. Letters 10, 392 (1963).
18. F. Stockmann, Z. Physik 143, 348 (1955).
19. R. H. Bube, Photoconductivity of Solids, John Wiley and Sons, New York (1960).
20. T. Ya. Sëra and G. G. Chemersoyuk, Sov. Phys. Solid State 6, 104 (1964).
21. T. Ya. Sëra, G. G. Chemersoyuk and V. N. Duldier, Sov. Phys. Solid State 6, 3015 (1965).

22. G. G. Chemeresyuk and V. V. Serdyuk, Sov. Phys. Semicond. 1, 320 (1967).

23. E. Gutsche, F. Spiegelberg, and J. Voigt, Phys. Stat. Sol. 17, K11 (1966).

Figure Captions

Figure 1. Effect of heat treatment on the 98°K SDP at $\sim 10^{-8}$ torr. Curve 1: virgin crystal; 2: 75°C heat treatment; 3: 125°C heat treatment; 4: 175°C heat treatment.
a) $\vec{E} \| \vec{C}$ b) $\vec{E}_{\perp} \vec{C}$

Figure 2. Effect of heat treatment on the 295°K SDP at $\sim 10^{-8}$ torr. $\vec{E} \| \vec{C}$ Curve 1: virgin crystal; 2: 75°C heat treatment; 3: 125°C heat treatment; 4: 175°C heat treatment.

Figure 3. Effect of heat treatment on the double beam excitation results at 98°K and 10^{-8} torr. Curve 1: virgin crystal; 2: 75°C heat treatment; 3) 125°C heat treatment; 4) 175°C heat treatment.
a) $\vec{E} \| \vec{C}$ b) $\vec{E}_{\perp} \vec{C}$

Figure 4. Effect of heat treatment on the double beam excitation results at 295°K and 10^{-8} torr. $\vec{E} \| \vec{C}$. Curve 1: virgin crystal; 2: 75°C heat treatment; 3: 125°C heat treatment; 4: 175°C heat treatment.

Figure 5. SDP at $\sim$ 87°K and $\sim 10^{-3}$ torr 1) before and 2) after heat treatment to 175°C.
a) $\vec{E} \| \vec{C}$ b) $\vec{E}_{\perp} \vec{C}$

Figure 6. SDP at 295°K and $\sim 10^{-3}$ torr 1) before and 2) after heat treatment to 175°C. $\vec{E} \| \vec{C}$.

Figure 7. Effect of 0.85 μm illumination on the SDP at $\sim$ 87°K and $\sim 10^{-3}$ torr. $\vec{E} \| \vec{C}$. Curve 1: without IR; 2) with IR.

Figure 8. Spectral distribution of the quenching of 1) the B-exciton photocurrent and 2) the near band edge photocurrent (4933 Å, $\vec{E} \perp \vec{C}$) at $\sim$ 87°K and 10^{-3} torr. Dashed lines represent the respective bias photocurrent levels.

Figure 9. Kinetic behavior of the excitation of the near band edge peak (4933 Å, $\vec{E} \perp \vec{C}$) at $\sim$ 87°K.

Figure 10. Band model of the active region of a Class I crystal.

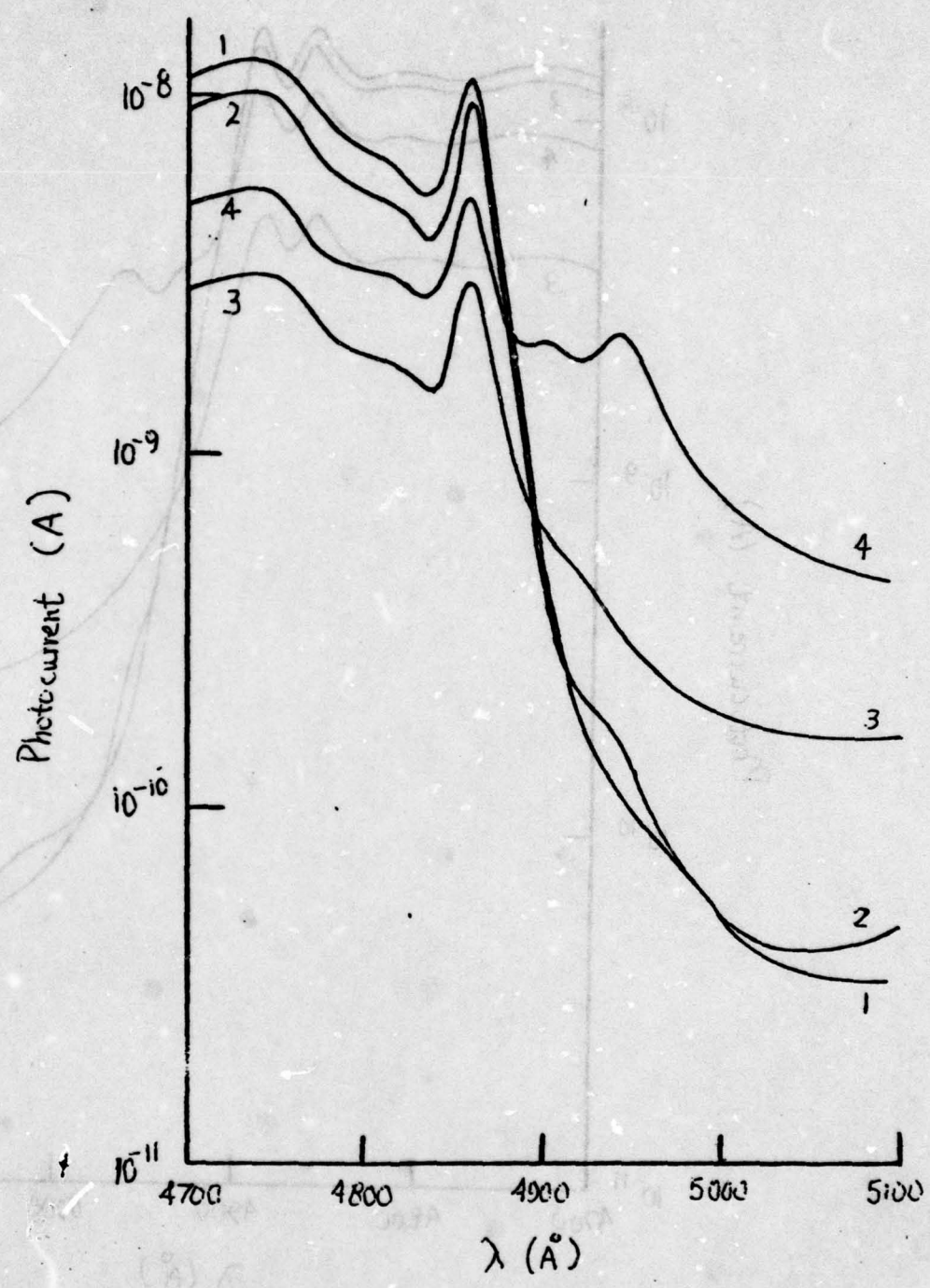
Photocurrent (A)
10^{-8}
10^{-9}
10^{-10}
10^{-11}
1
2
4
3
4
3
2
1
4700
4800
4900
5000
5100
λ (Å)

Fig. 1a.

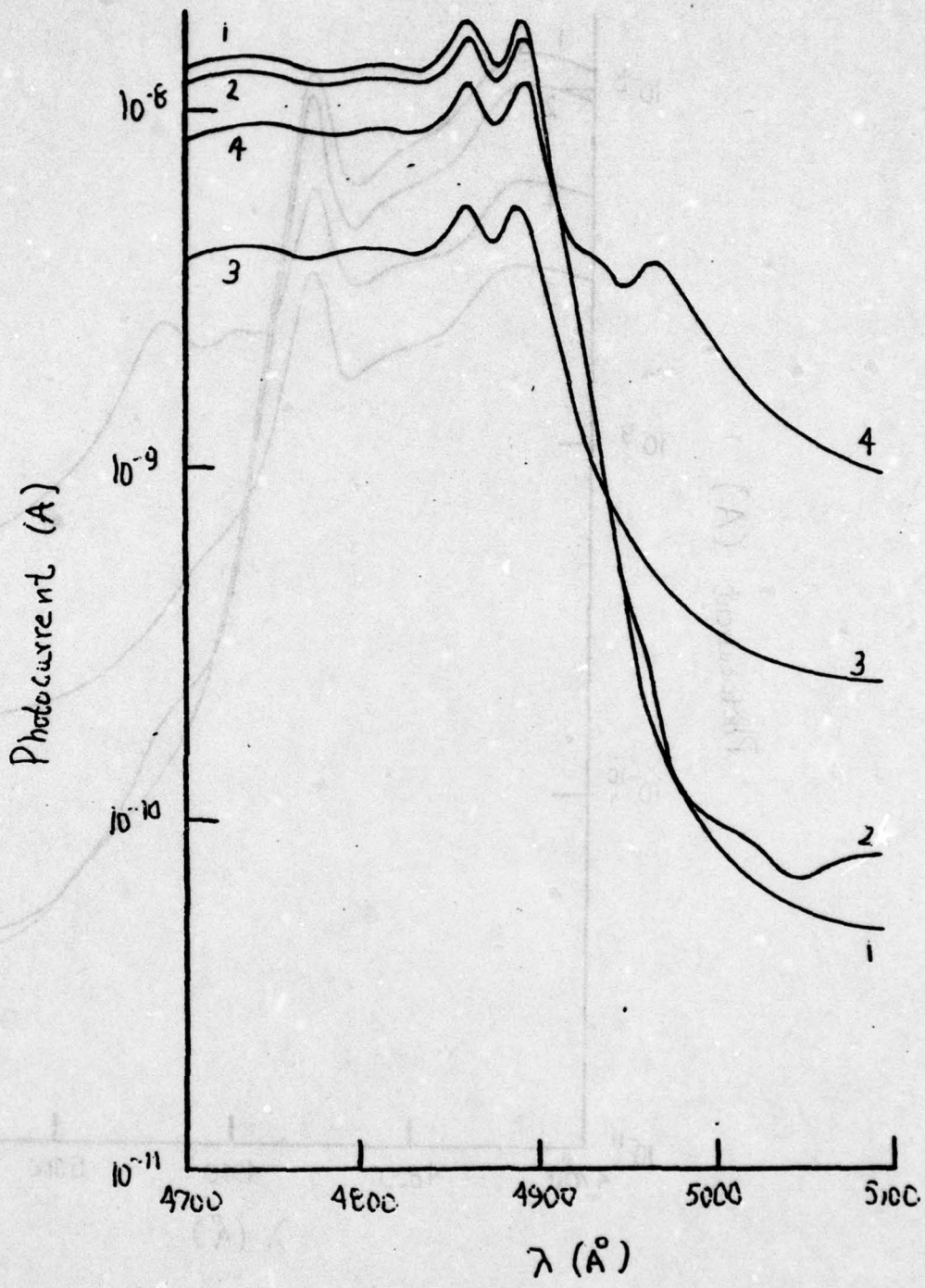
Photocurrent (A)
10^{-8}
10^{-9}
10^{-10}
10^{-11}
4700
4800
4900
5000
5100
λ (Å)
1
2
3
4
1
2
3
4

Figure 1b.

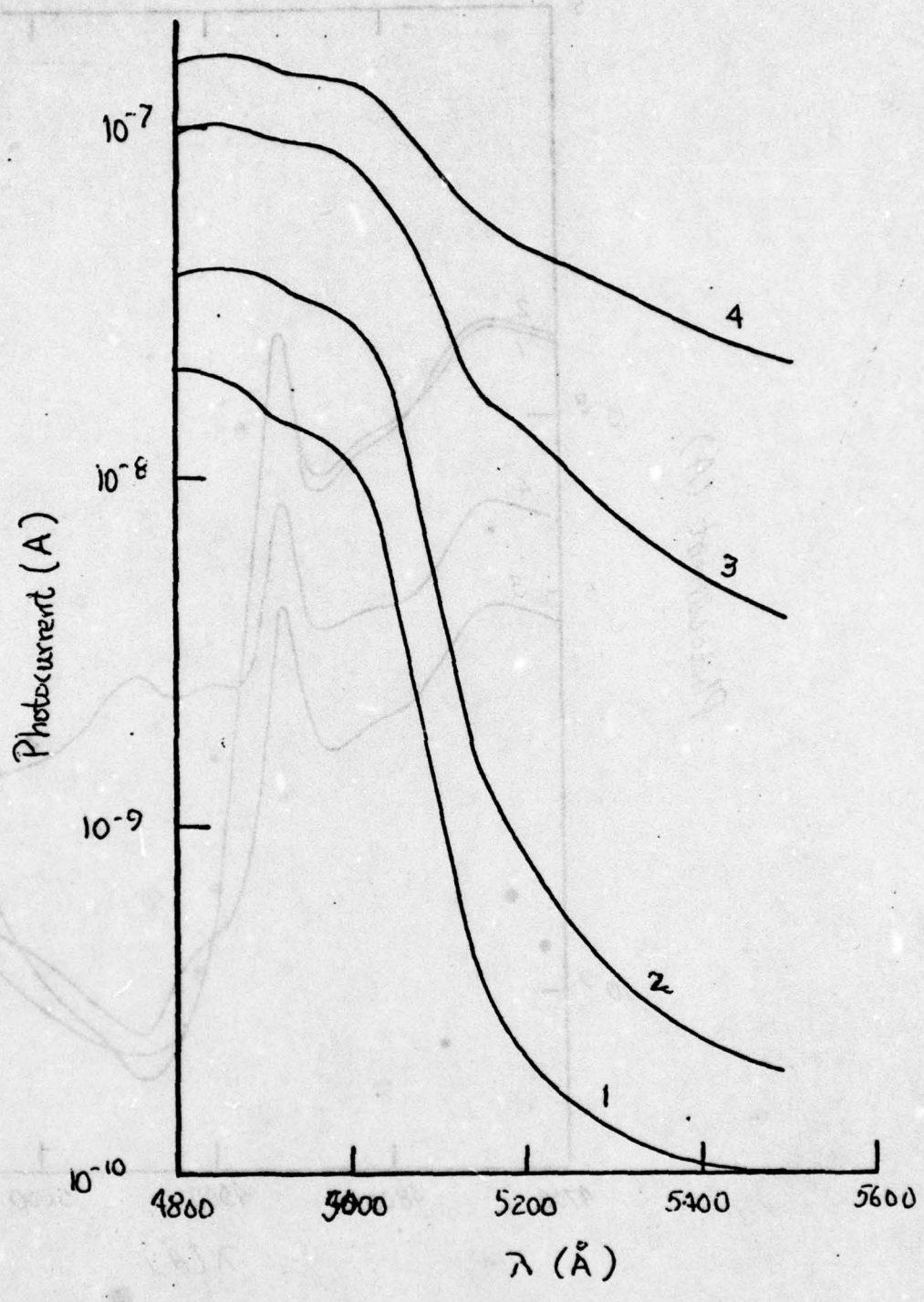
Photocurrent (A)
10⁻⁷
10⁻⁸
10⁻⁹
10⁻¹⁰
4800
5000
5200
5400
5600
λ (Å)
1
2
3
4

Figure 2.

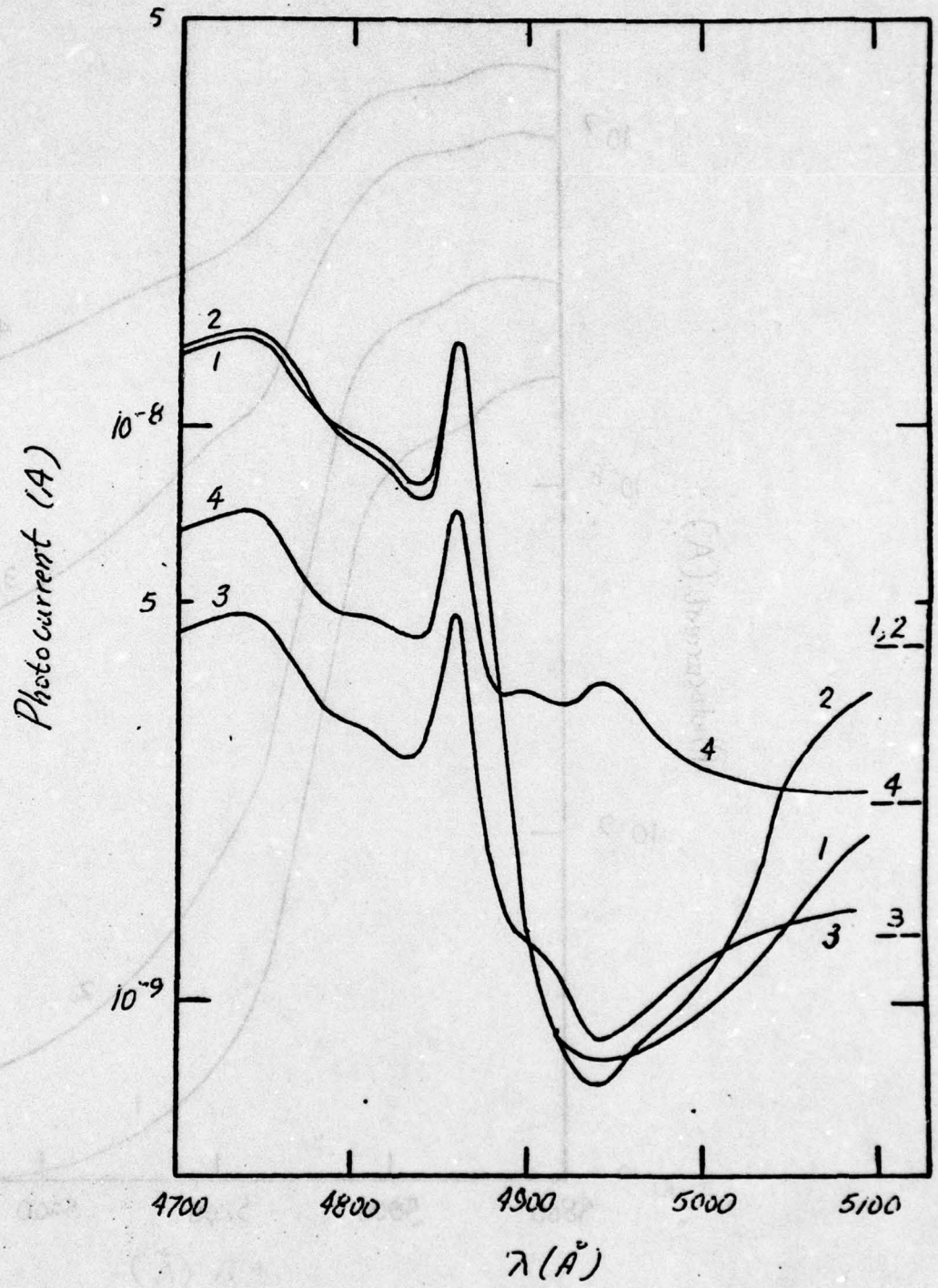
5
2
1
10^{-8}
4
5
3
Photocurrent (A)
1,2
2
4
4
1
3
3
10^{-9}
4700
4800
4900
5000
5100
λ (Å)

Figure 3a.

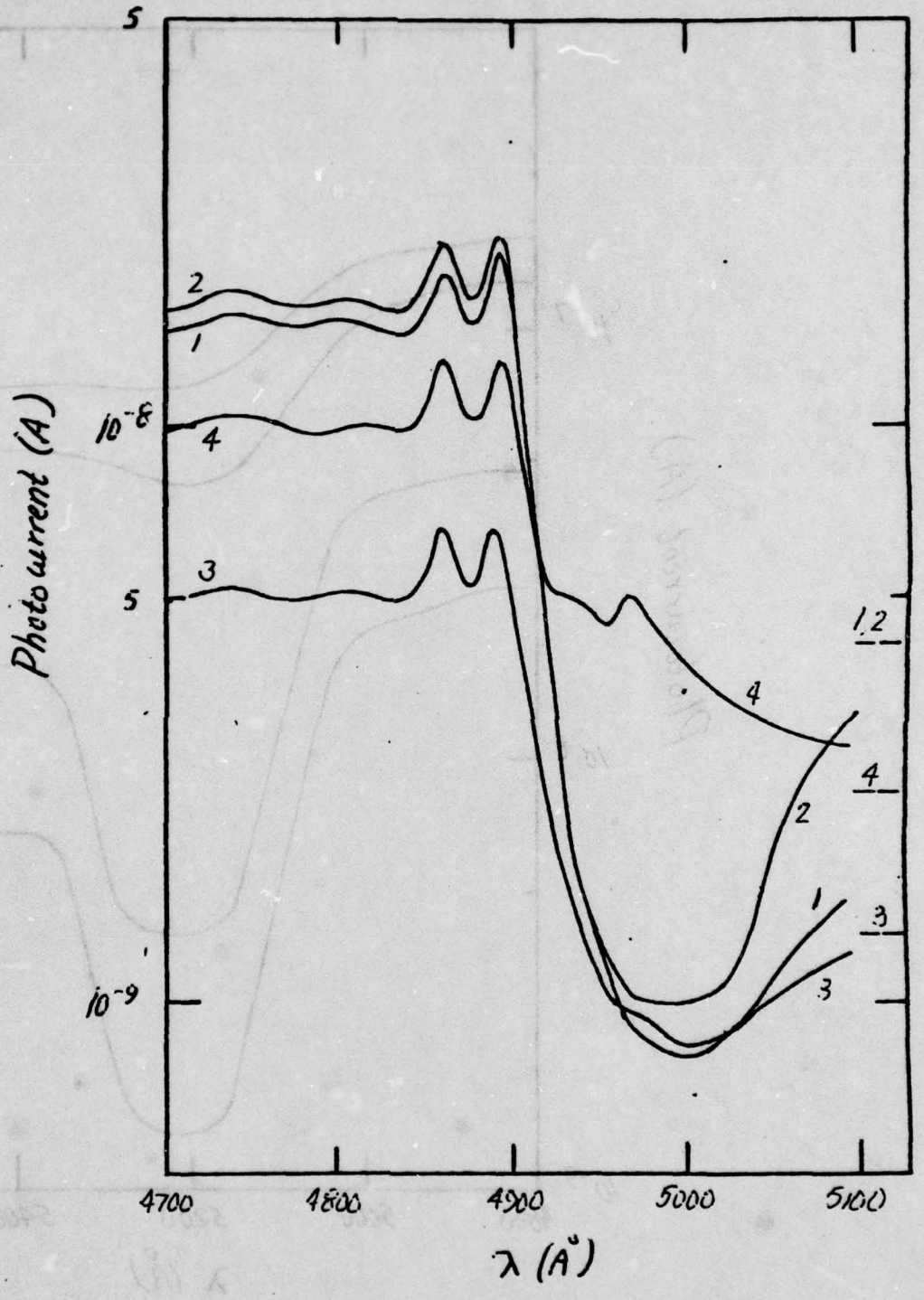
5
2
1
10^{-8}
4
3
5
Photo current (A)
1.2
4
4
2
1
3
3
10^{-9}
4700
4800
4900
5000
5100
λ (Å)

Figure 3b.

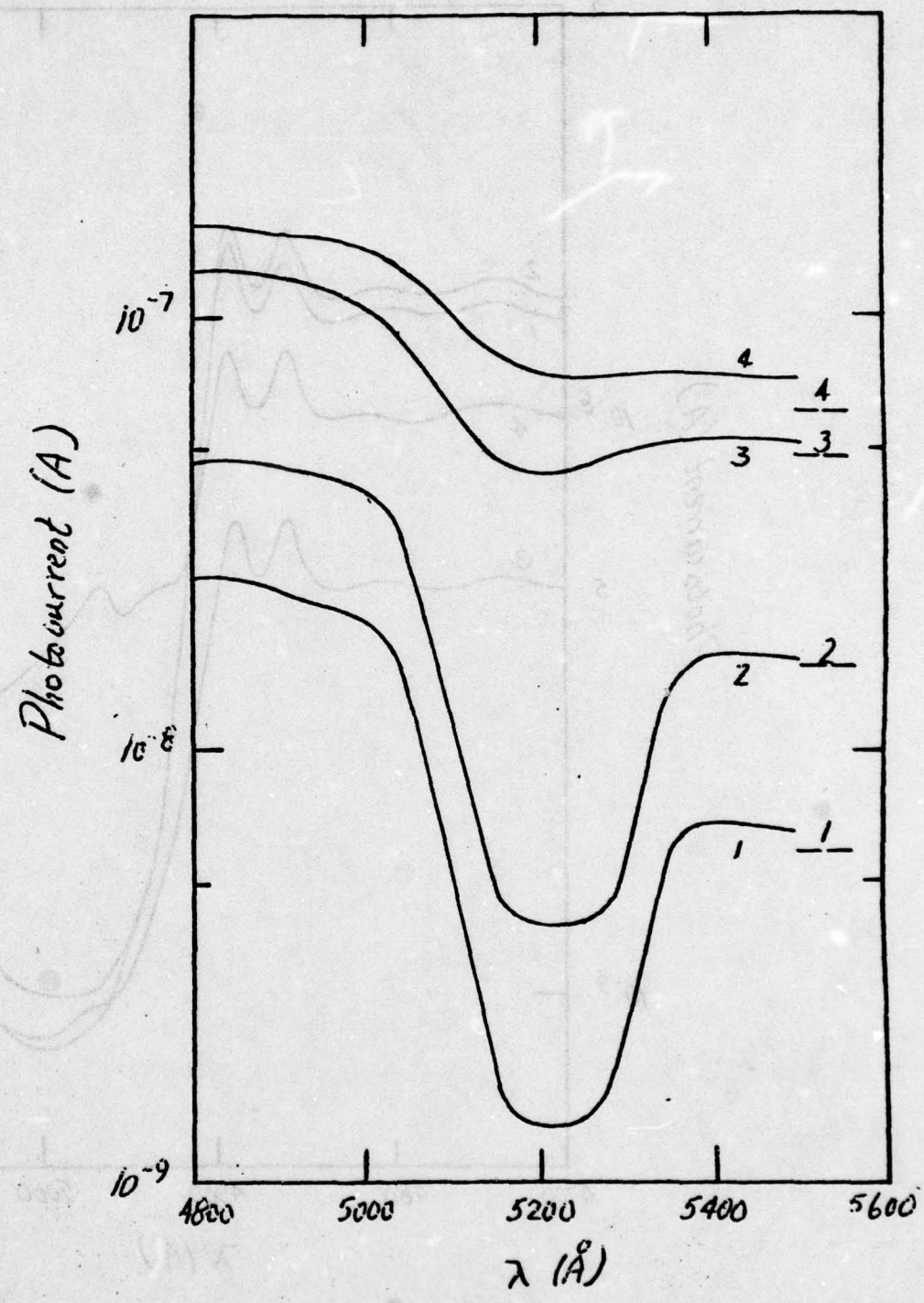
Photocurrent (A)
10^{-7}
10^{-8}
10^{-9}
4
4
3
3
2
2
1
1
4800
5000
5200
5400
5600
λ (Å)

Figure 4.

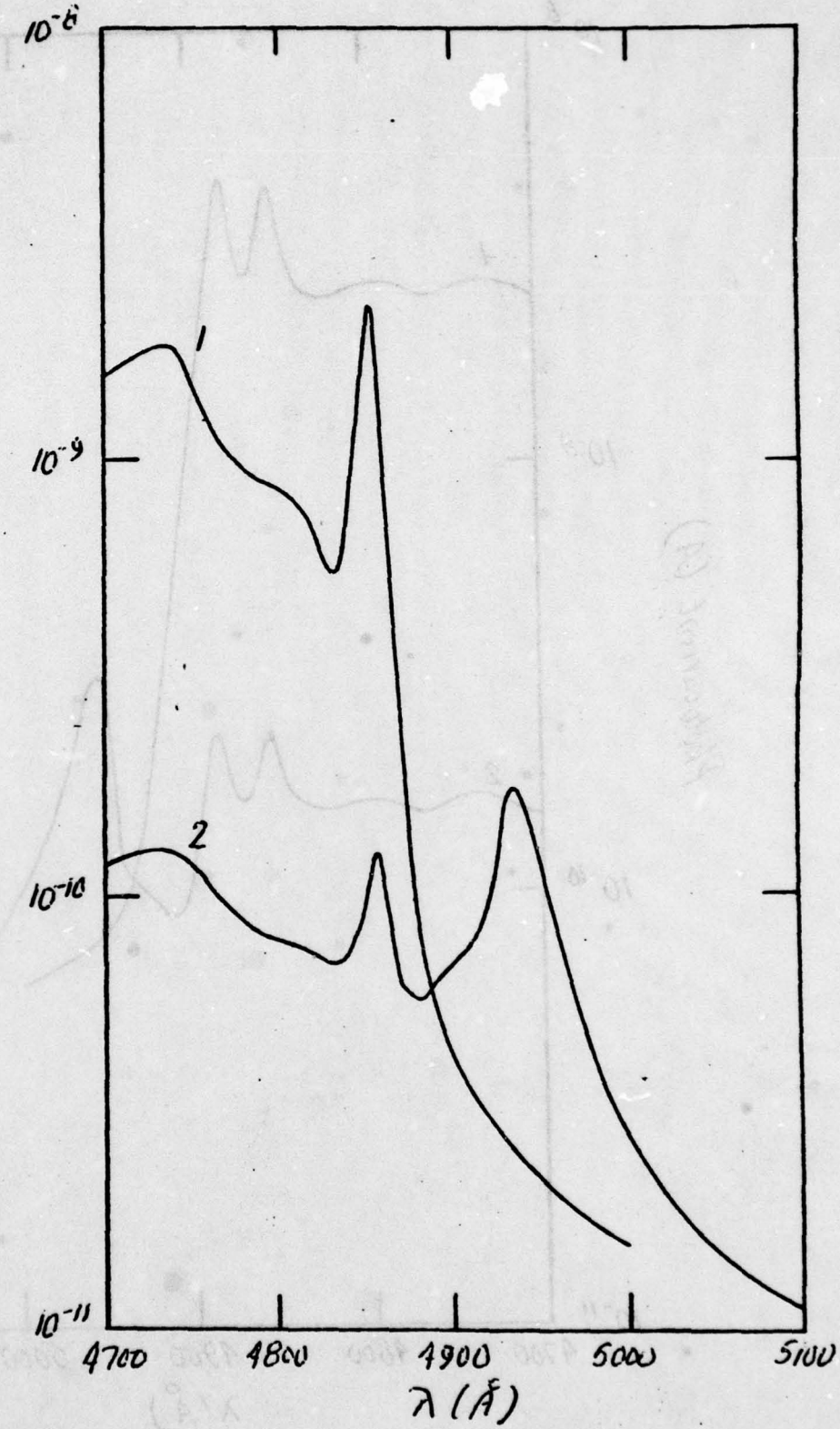
10^{-8}
10^{-9}
10^{-10}
10^{-11}
Photocurrent (A)
1
2
4700
4800
4900
5000
5100
λ (Å)

Figure 5a.

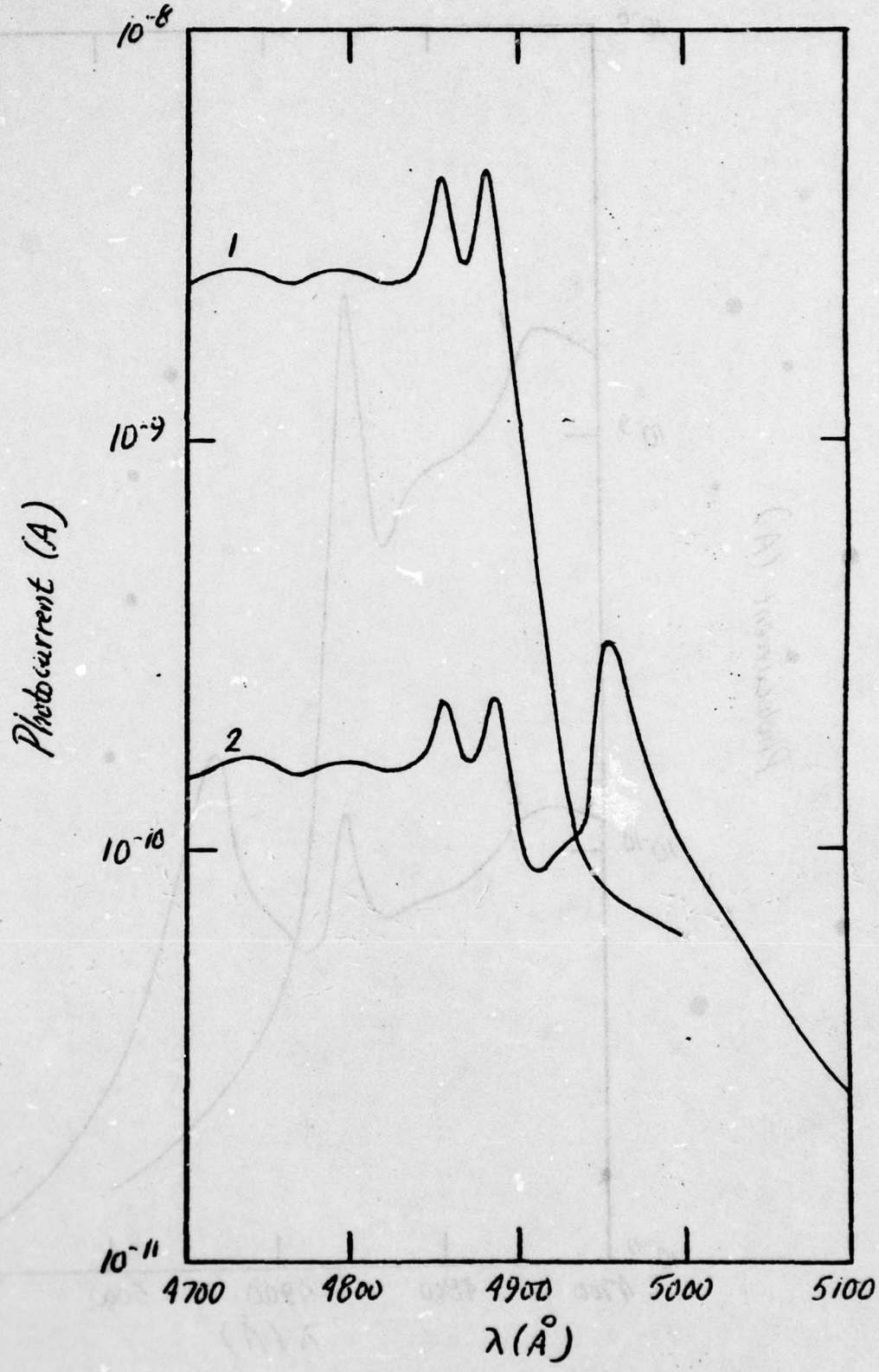
10^{-8}
10^{-9}
10^{-10}
10^{-11}
Photocurrent (A)
1
2
4700
4800
4900
5000
5100
λ(Å)

Figure 5b.

5b

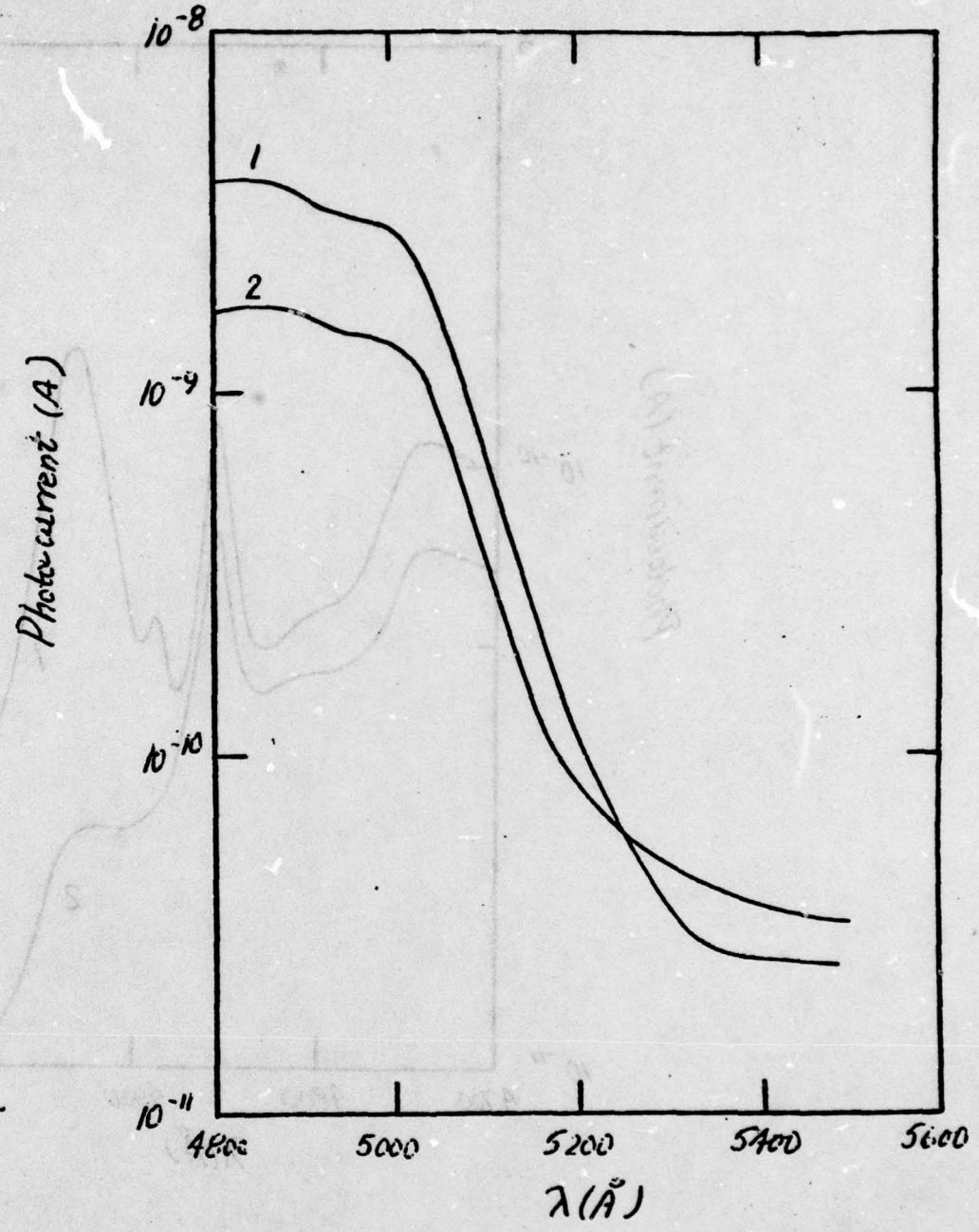
10^{-8}
10^{-9}
10^{-10}
10^{-11}
1
2
Photocurrent (A)
4800
5000
5200
5400
5600
λ(Å)

Figure 6.

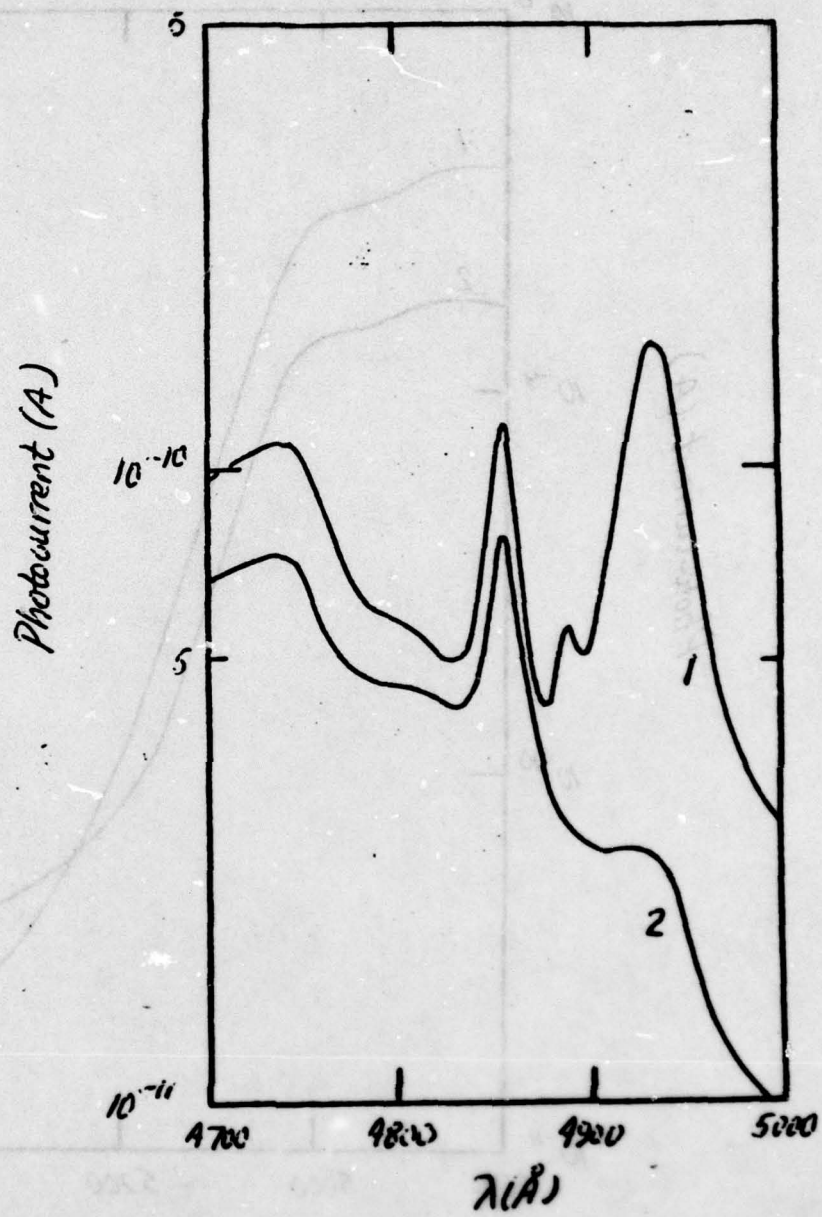

Figure 7

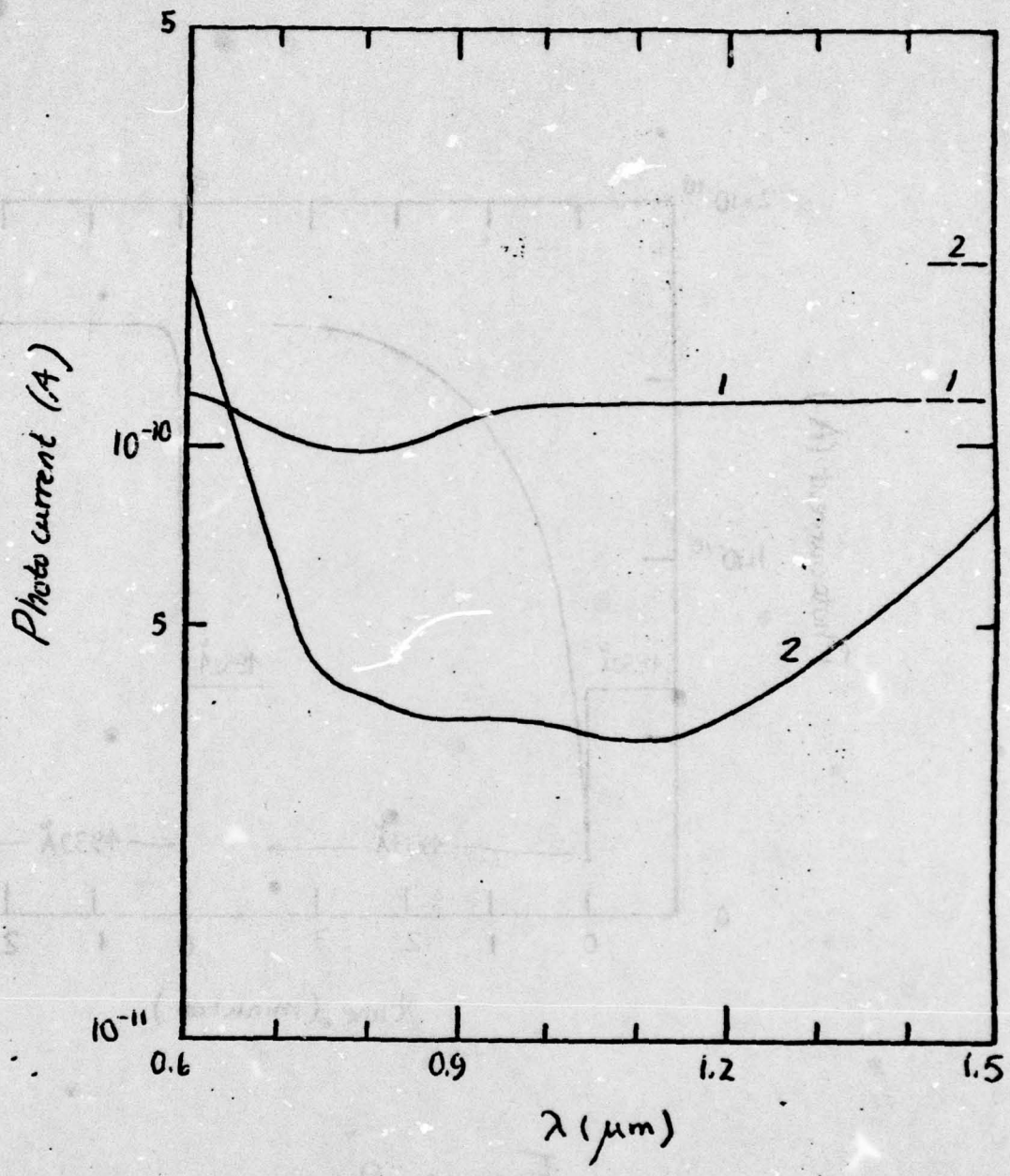

Figure 8.

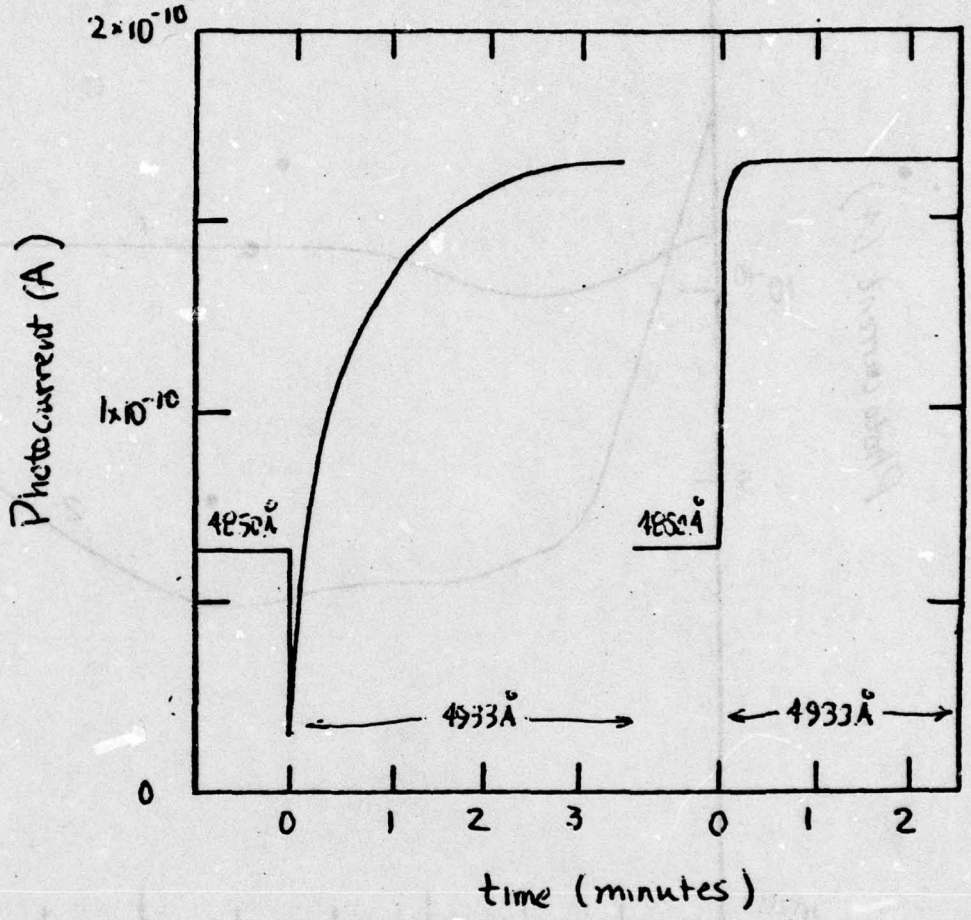
2×10⁻¹⁰
1×10⁻¹⁰
0
Photocurrent (A)
4850Å
4850Å
4933Å
4933Å
0
1
2
3
0
1
2
time (minutes)

Figure 9.

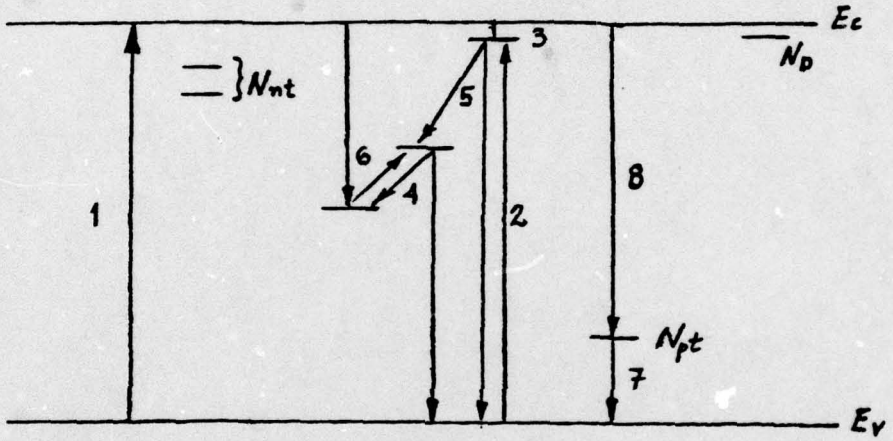
E_c
N_D
N_{nt}
3
5
6
4
1
2
8
N_{pt}
7
E_v
0 -1 -2
CHARGE STATE
OF
MULTI-CHARGED
RECOMBINATION
CENTER